Biophysical Journal Volume 107 November 2014 2027–2036

Article

Monovalent Cationic Channel Activity in the Inner Membrane of Nuclei from Skeletal Muscle Fibers

Viktor Yarotskyy[1,*] and Robert T. Dirksen[1]

[1]Department of Pharmacology and Physiology, University of Rochester Medical Center, Rochester, New York

ABSTRACT Nuclear ion channels remain among the least studied and biophysically characterized channels. Although considerable progress has been made in characterizing calcium release channels in the nuclear membrane, very little is known regarding the properties of nuclear monovalent cationic channels. Here, we describe a method to isolate nuclei from adult skeletal muscle fibers that are suitable for electrophysiological experiments. Using this approach, we show for the first time, to our knowledge, that a nuclear monovalent cationic channel (NMCC) is prominently expressed in the inner membrane of nuclei isolated from flexor digitorum brevis skeletal muscle fibers of adult mice. In isotonic 140 mM KCl, the skeletal muscle NMCC exhibits a unitary conductance of ~160 pS and high, voltage-independent open probability. Based on single-channel reversal potential measurements, NMCCs are slightly more permeable to potassium ions over sodium (P_K/P_{Na} = 2.68 ± 0.21) and cesium (P_K/P_{Cs} = 1.39 ± 0.03) ions. In addition, NMCCs do not permeate divalent cations, are inhibited by calcium ions, and demonstrate weak rectification in asymmetric Ca^{2+}-containing solutions. Together, these studies characterize a voltage-independent NMCC in skeletal muscle, the properties of which are ideally suited to serve as a countercurrent mechanism during calcium release from the nuclear envelope.

INTRODUCTION

The cell nucleus is a unique organelle enclosed by a complex structure called the nuclear envelope. The nuclear envelope consists of two membranes (1,2) and nuclear pore complexes (NPCs) that physically link the cytoplasm and nucleoplasm (1–4). This structure serves at least two functions: 1), to protect the genetic apparatus (barrier function) and 2), to provide ionic and macromolecular (e.g., RNAs, transcription factors, sugars, etc.) exchange between the cytoplasm and nucleoplasm via NPCs (transport function) (4,5). Early electron microscopy studies revealed that the inner and outer nuclear membranes exhibit distinct ultrastructures (6,7), suggesting specific roles for the two membranes. A third function of the nuclear envelope as a calcium storage and release compartment has recently emerged. Indeed, the perinuclear space between the inner and outer membranes provides a storage of Ca^{2+} ions that can be released upon opening of Ca^{2+} release channels located within the nuclear envelop (8–14). Electrophysiological studies have confirmed the presence of inositol 1,4,5-trisphosphate (IP_3)-gated channels (15–21), and more recently, ryanodine-sensitive Ca^{2+} release channels (22,23) in the nuclear envelope. In addition, small conductance channels permeable to Ca^{2+} and Zn^{2+} ions were reported in nuclei from rat hepatocytes (24).

Along with Ca^{2+}-permeable channels, other nuclear cationic and anionic channels have also been reported (15,25–29). Although nuclear Ca^{2+} release channels increase local nucleoplasmic and/or cytoplasmic Ca^{2+} concentrations to activate Ca^{2+}-dependent events (8–10,14,15,18,19,30), the physiological roles of other nuclear ion channels likely depend on context including channel properties, cell type, nuclear membrane localization, cell cycle stage, etc. For example, nuclear chloride channel 27 (NCC27) regulate the cell cycle (31) and K_V10.1 channels in the inner nuclear membrane influence cancerogenesis through alterations in gene expression (27). In addition, both cationic (potassium) and anionic (chloride) channels control monovalent ion exchange between the cyto/nucleoplasm and perinuclear space, which serves to counteract the development of charge imbalance between these two compartments (15,25,26,32).

Nuclei in adult skeletal muscle are primarily located on the periphery of the muscle fiber, nestled in close proximity to the muscle fiber plasma membrane. This intimate coupling between the nucleus and plasma membrane in skeletal muscle enables efficient signal transmission from the surface membrane to the nucleoplasm and transcriptional machinery (33–36). However, the precise role of nuclear ion channels in regulating skeletal muscle signaling, growth, development, and gene transcription is largely unknown. Knowledge regarding nuclear ion channels in skeletal muscle is limited to the detection of IP_3-sensitive channels from external and internal nuclear membranes of immature 1B5 myotubes (21). However, 1B5 myotubes lack ryanodine receptors (RyRs), which are the primary intracellular Ca^{2+} release channel in skeletal muscle.

Submitted April 8, 2014, and accepted for publication September 30, 2014.

*Correspondence: Viktor_Yarotskyy@URMC.Rochester.edu

Editor: Miriam Goodman.

0006-3495/14/11/2027/10 $2.00

http://dx.doi.org/10.1016/j.bpj.2014.09.030

Indeed, a severe reduction in type 1 RyR activity results in mutliminicore disease, an inheritable myopathy characterized by the presence of multiple, short-length amorphous regions that lack mitochondria and oxidative enzymatic activity (37). In addition, recent findings show that IP_3 signaling is less prominent in adult skeletal muscle fibers compared to immature myotubes (38). However, osmotic stress transiently triggers prominent peripheral Ca^{2+} sparks that occur as a result of cross talk between type I IP_3 receptors (IP_3Rs) and type I RyRs (39). Given the peripheral localization of osmotic shock-induced Ca^{2+} sparks, it is plausible that the IP_3Rs are actually nuclear receptors (40). Nevertheless, ion channels expressed in nuclei isolated from adult muscle may differ significantly from that observed in cultured myotubes.

Here, we describe a method to isolate nuclei from adult skeletal muscle fibers that are suitable for electrophysiological characterization of ion channels located within the inner nuclear membrane. Using this approach, we confirmed the presence of high-conductance, IP_3-responsive channels in the inner nuclear membrane and characterized the single-channel properties of a high conductance, voltage-independent, monovalent cation channel that is widely expressed in the inner nuclear membrane (NMCC). The NMCC exhibits a voltage-independent high open probability, modest calcium-dependent rectification, preference for potassium permeation over sodium and cesium, and is impermeant to, and inhibited by, calcium ions. These properties are consistent with NMCCs serving as a nuclear countercurrent channel that limits charge imbalance across the nuclear membrane during Ca^{2+} release through IP_3Rs and/or RyRs.

METHODS

Ethical approval

All animals were housed in a pathogen-free area at the University of Rochester and all experiments were carried out in accordance with procedures reviewed and approved by the University of Rochester University Committee on Animal Resources. Mice were sacrificed by a regulated overdose delivery of compressed CO_2 followed by decapitation.

Isolation and plating of nuclei

Isolation of nuclei was based on a two-step procedure that consisted of isolation of single muscle fibers followed by liberation of nuclei. Single muscle fibers were isolated from the *flexor digitorum brevis* (FDB) muscle as described previously (41). Briefly, FDB muscle of 3-week- to 4-month-old C57Bl6 mice was cleaned of connective tissues, removed from the food pad, and enzymatically digested in a Rodent Ringer solution consisting of (mM): 145 NaCl, 5 KCl, 2 $CaCl_2$, 1 $MgCl_2$, 10 HEPES, pH 7.4, and supplemented with 1 mg/ml collagenase A (Roche Diagnostics, Indianapolis, IN) while gently shaking for 30–45 min at 37°C. The FDB muscle was then washed twice with a Ca^{2+}-free rodent Ringer solution consisting of (mM): 145 NaCl, 5 KCl, 1 $MgCl_2$, 10 HEPES, 0.2 EGTA, pH 7.4, and transferred into a 15 ml tube containing 2 ml isolation solution formulated by adding a manufacturer's recommended amount of Halt Protease Inhibitor Cocktail (100×) (Thermo Fisher Scientific, Waltham, MA), 0.2 mM phenylmethanesulfonylfluoride, and 3.5 mM mercaptoethanol to the Ca^{2+}-free rodent Ringer solution. FDB muscles were then triturated with a fire polished Pasteur pipette until single muscle fibers were liberated. Single FDB fibers were then carefully transferred to an ice-chilled 8 ml Dounce homogenizer and nuclei were released into isolation solution after 20–25 strokes.

In some experiments, the isolation was simplified by skipping the collagenase A digestion step and FDB muscles were directly homogenized in isolation solution using a Tissumizer TR-10 homogenizer (Tekmar, Cincinnati, OH) at 12,000 rpm for 5–7 s at 4°C. Nuclei from FDB fibers were of similar size, shape, translucency, and surface morphology regardless of the method of isolation. Of importance, NMCC activity was not different between the two isolation procedures.

To render the inner membrane accessible for patch clamp, we used a method similar to that described previously (15,26,30). Briefly, 1% (w/v) sodium citrate was added to the crude homogenate for at least 1 h at 4°C while stirring gently. Sodium citrate treatment resulted in removal of the outer membrane enabling patch pipette access to the inner membrane from the perinuclear side of the nuclear envelope.

Treated nuclei were then plated into 35-mm plastic dishes, which also served as recording chambers. Treatment with sodium citrate significantly improved adhesion of nuclei to the bottom of the dishes. Thus, excised patches from the inner membrane were routinely obtained even in the absence of dish coating adhesives such as poly-D-lysine or poly-L-lysine. After plating, nuclei were washed twice with bath solution to remove debris.

Immunofluorescence labeling

Potential contamination of isolated nuclei with remnants of the sarcoplasmic reticulum (SR) was tested by immunofluorescent labeling of triadin as described previously (42). A rabbit C-terminal specific (residues 691–706) antitriadin antibody (1:10000, generously donated by Dr. I. Marty) was used to detect triadin (43) in both intact FDB fibers and isolated nuclei. A fluorescent Alexa Fluor 488-labeled goat antirabbit secondary IgG (1:500, Molecular Probes) was used to detect the triadin primary antibody.

Electrophysiology

Single-channel activity was recorded from excised nuclear patches. Patch pipettes were fabricated from borosilicate glass with a trough filament (Sutter Instruments, Novato, CA) and were filled, unless otherwise stated, with a pipette recording solution consisting of (mM): 140 KCl, 10 mM $CaCl_2$, 10 HEPES, pH 7.4. Pipette resistances in the bath ranged from 10 to 25 MΩ. The bath recording solution was made by adding 1 mM EGTA and 0.95 mM $CaCl_2$ (1.2 μM free Ca^{2+} Ca^{2+} calculated using MaxChelator; http://maxchelator.stanford.edu/) to a base solution consisting of 140 KCl, 10 HEPES, pH 7.4. Ion replacement studies were conducted in individual excised patches in which K^+ ions were replaced by other cations (e.g., Na^+, Cs^+, Ca^{2+}). For IP_3-sensitive channels, recordings were made using symmetric solutions consisting of (in mM) 140 KCl, 10 HEPES, 0.5 Na_2-ATP, 0.53 K_2EGTA, 1.47 CaEGTA (300 nM free Ca^{2+}), pH 7.3. To avoid confusion caused by channel orientation in nuclear membranes, all potentials reported here represent pipette potentials. An electrode connected to the bath solution via a 3 M KCl agar bridge was used to minimize the effect of ion exchange on the pipette potential. Single-channel currents were recorded using an Axopatch 200A amplifier (Molecular Devices, Sunnyvale, CA), filtered at 5 kHz using an inline four-pole Bessel filter and data were digitized at 10 kHz using a DigiData 1200 interface (Molecular Devices). All recordings were obtained at room temperature (21–23°C).

Offline data analysis

All single-channel analyses were performed using Igor (Wavemetrics, Lake Oswego, OR) and Clampfit10 (Molecular Devices) software. Original

recordings were filtered offline using a low-pass Bessel filter at 1 kHz. Single-channel current amplitudes were determined by plotting current histograms and measuring the difference between two neighboring peaks of the current amplitude normal distributions reflecting the fully closed and opened states. Open probability was determined by integrating the open durations over the total duration of a recording at a given pipette potential. The total duration was chosen in a range from 15 to 120 s with the median value equal to 26 s. The permeability ratio P_K/P_X, where X refers to the permeability of ion X, was calculated as previously described (15).

The fractional inhibition of NMCC conductance was calculated as a ratio of the difference between the average maximal conductance measured in symmetrical zero Ca^{2+} solutions and measured conductance to the average maximal conductance measured in symmetrical zero Ca^{2+} solutions. Assuming that NMCC is not permeable to Ca^{2+} ions, calculated values were then fitted by the following standard Hill equation:

$$\text{Fractional Inhibition of Conductance} = \frac{1}{1+\left(\frac{[Ca]_{0.5}}{[Ca]}\right)^{n}},$$

where [Ca] is the bath Ca^{2+} concentration, $[Ca]_{0.5}$ is the half-maximum bath Ca^{2+} concentration, and n is the Hill coefficient.

Group data were calculated as means ± SE throughout the work. In the majority of figures summarizing the voltage-dependences of mean (± SE) single-channel current amplitude, the SE bars are smaller than symbol sizes. A Student's two-tailed *t*- test was used for two independent group data comparisons. One-way ANOVA with Tukey's HSD post hoc test was used to test for differences among three or more independent groups.

Chemicals

D-*myo*-Inositol 1,4,5-trisphosphate hexapotassium salt (IP_3) was purchased from Tocris (Ellisville, MO). All other chemicals were purchased from Sigma-Aldrich (St. Louis, MO).

RESULTS

Isolation and identification of nuclei from FDB fibers

As crude muscle homogenates could be contaminated by nuclei from nonmuscle cells, liberated nuclei used for electrophysiological recordings were carefully compared to the size, shape, color, and relative translucency of that observed for nuclei in intact FDB muscle fibers. Initial identification of isolated nuclei was achieved by comparing Hoechst-stained nuclei in intact FDB fibers with similarly stained nuclei liberated from crude muscle homogenates. Nuclei in intact fibers and free nuclei from muscle homogenates exhibited similar size, shape, color, and relative translucency. Fig. 1 illustrates the similarity that exists between confocal images of nuclei from both groups. In both cases, Hoechst-stained nuclei were identified as ellipsoid objects with length/width ratio varying from 2.4 to 4.2. Liberated nuclei were further investigated under brightfield to confirm muscle nuclei shape/size parameters by color, surface morphology, and translucency. Nuclei isolated from FDB fibers were also similar to those isolated from *tibialis anterior* muscle (data not shown), further confirming their identity as muscle-derived nuclei.

Detection of IP_3R activity as confirmation of inner nuclear membrane accessibility for patch clamp recording

There are no reports describing the properties of ion channels in nuclei isolated from adult skeletal muscle. Thus, initial experiments involved the most direct approach: detection of single-channel activity in inner membrane patches excised from nuclei isolated from FDB muscle of adult mice. The success rate of achieving gigaohm seals and detecting single-channel activity of some type in excised nuclear patches varied widely from 20% to 100% depending on the preparation of nuclei, which most likely reflected a quality of nuclei in the isolation (e.g., total number of isolated nuclei, fraction of mechanically damaged nuclei, inner membrane accessibility, etc.).

Despite wide acceptance of sodium citrate treatment as an efficient method of rendering the inner membrane accessible for patch pipette (15,26,30,44), this approach has not

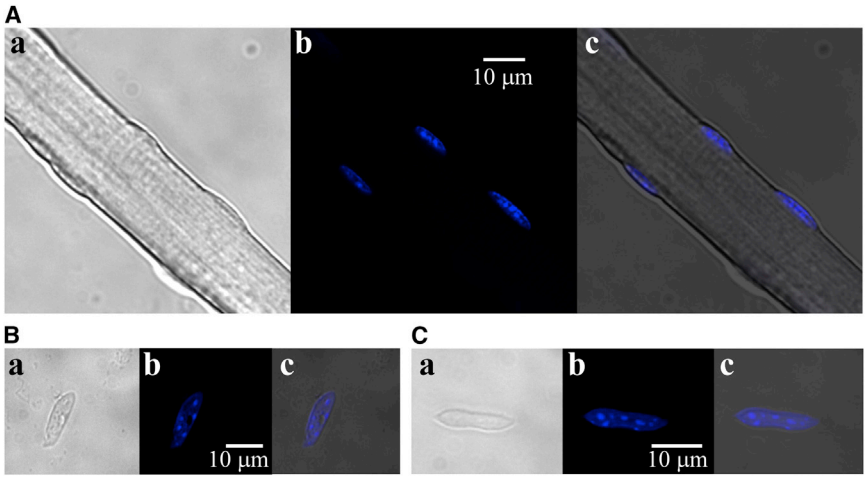

FIGURE 1 Representative images of skeletal muscle nuclei. (*A*) Three nuclei are localized at the periphery of a single FDB fiber. (*a*) Brightfield image; (*b*) Confocal image (nuclei stained with Hoechst 34580); (*c*) Merged image of (*a*) and (*b*). (*B* and *C*) Representative brightfield (*a*), confocal (*b*), and merged (*c*) images of single nuclei following isolation from FDB fibers.

been validated for nuclei isolated from skeletal muscle fibers. Thus, we used 1 μM IP_3 added to the bath solution to activate IP_3R channels in the nuclear inner membrane because IP_3 cannot penetrate nuclear membranes. Thus, the presence of IP_3 in the bath solution will activate IP_3Rs only when recorded from seals obtained from excised inner nuclear membrane patches where the nucleoplasmic side of the channel is facing the bath recording solution. Fig. 2 illustrates the opening of a 325 pS conductance channel upon bath application of 1 μM IP_3, consistent with the activity of nuclear IP_3R channels recorded previously (15,18,45,46). The frequency of observing IP_3R channel activity was low (2 out of 113 patches, or ~2%), which is consistent with weak IP_3 signaling in FDB fibers from adult skeletal muscle (38). The low frequency of detecting IP_3 receptor channels in these experiments could potentially reflect contamination of the nuclear preparation with remnants of the SR. Therefore, immunofluorescence labeling of triadin was used to check whether the nuclei preparation was significantly contaminated with remnants of the terminal SR. The results revealed extremely weak triadin staining in the nuclear membrane in both isolated nuclei (Fig. S1 *A* in the Supporting Material) and intact muscle fibers (Fig. S1 *B*), whereas robust double-row staining, consistent with junctional triadin expression, was observed within the FDB fiber interior. Thus, detection of IP_3R channel activity in isolated muscle nuclei following sodium citrate treatment confirmed the accessibility of the inner membrane for patch clamp experiments under these conditions.

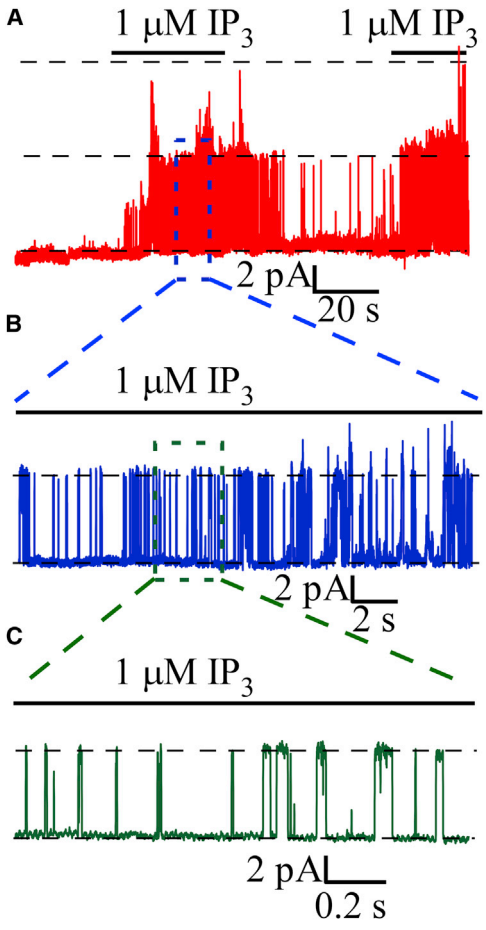

FIGURE 2 Addition of 1 μM IP_3 in the bath solution triggers IP_3R activity. (*A*) Application of IP_3 activates large conductance channel activity in a reversible manner. Channel activity was recorded at +20 mV. Horizontal bars show drug application times and durations. Dotted lines reflect closed and open state conductance levels. (*B*) Segment of the trace from the blue dashed box of panel *A* illustrating typical IP_3R gating at an expanded time base. (*C*) Segment of the trace from the green dashed box of panel *B* illustrating individual IP_3R openings and closings at a further expanded time base.

Single-channel activity in the inner nuclear membrane

Unlike IP_3R channels, the activity of a smaller conductance channel was detected frequently in isolated nuclei (143 out of 228 patches, or ~64%). Using our standard pipette and bath solutions (see Methods), this single-channel activity was observed in the absence of IP_3, exhibited a modestly inwardly rectifying voltage dependence (see Fig. 3 *B*), prolonged channel openings across a wide voltage range (from −50 to 50 mV; Fig. 3, *A* and *C*), and a unitary conductance of 158 ± 7 pS (n = 21). In addition, these channels exhibited a markedly high, voltage-independent mean open

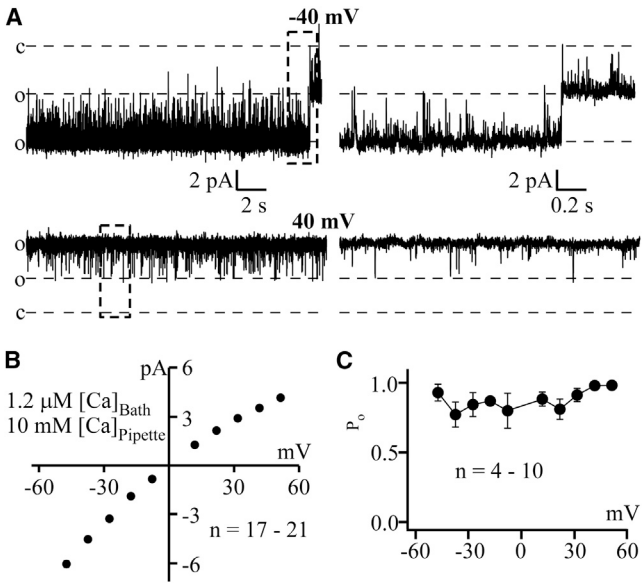

FIGURE 3 Channel activity in the inner nuclear membrane. (*A*) Representative traces of channel activity recorded at −40 mV (*top*) and 40 mV (*bottom*) pipette potentials. Traces shown on the right side of the panel are expanded regions of the traces on the left (as indicated by *dashed boxes*). (*B*) Average (±SE) i-V relationships were obtained by plotting unitary channel current amplitude against pipette voltage. (*C*) Average (±SE) open probability (P_o) collected from channels recorded from the inner nuclear membrane.

probability (P_o) (Fig. 3 *C*). Thus, these channels dwell in open state most of the time.

To determine relative ion permeation through the ~158 pS channel under these conditions (i.e., K^+ or Cl^-), the concentration of KCl in the bath recording solution was reduced from 140 to 70 mM while maintaining the pipette solution at 140 mM. This reduction in bath KCl concentration resulted in a leftward shift (-16.8 ± 0.6 mV, $n = 5$) of the linearly extrapolated single-channel reversal potential (Fig. 4). The most likely explanation for the leftward shift in reversal potential is that the current through the 158 pS channel predominantly reflects the permeation of potassium ions (cationic).

Large monovalent and divalent cations do not permeate the 158 pS channel

Our experiments demonstrated that large monovalent cations, such as *N*-methyl-D-glucamine ($NMDG^+$), do not permeate the channel ($n = 5$, Fig. 5 *A*). The absence of $NMDG^+$ permeation, the relatively small unitary conductance, and the cationic-selective nature of the channel ruled out the possibility of these channels reflecting NPC permeability (4,5,26).

We next tested the relative permeability of the channel to calcium, a small divalent cation. For these experiments,

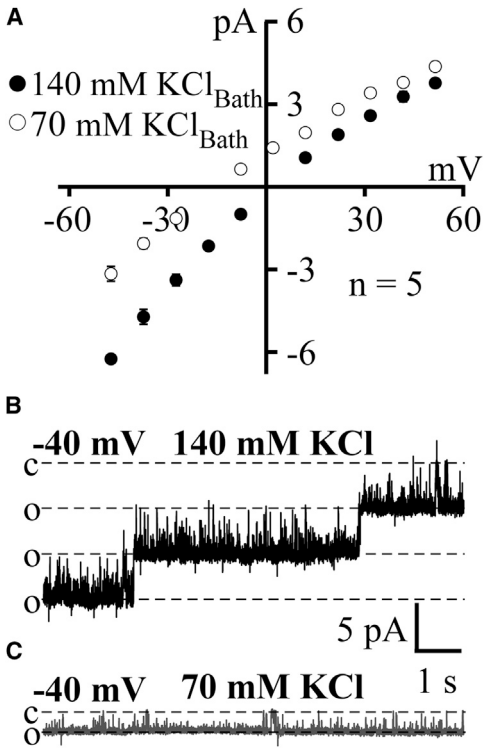

FIGURE 4 K^+ selectivity. (*A*) Average ($\pm$SE) i-V relationships in the presence of either 140 mM KCl (*solid circles*) or 70 mM KCl (*open circles*) in the bath recording solution. (*B* and *C*) Representative channel traces recorded at -40 mV pipette potential in bath solutions containing 140 mM KCl (*B*) and 70 mM KCl (*C*).

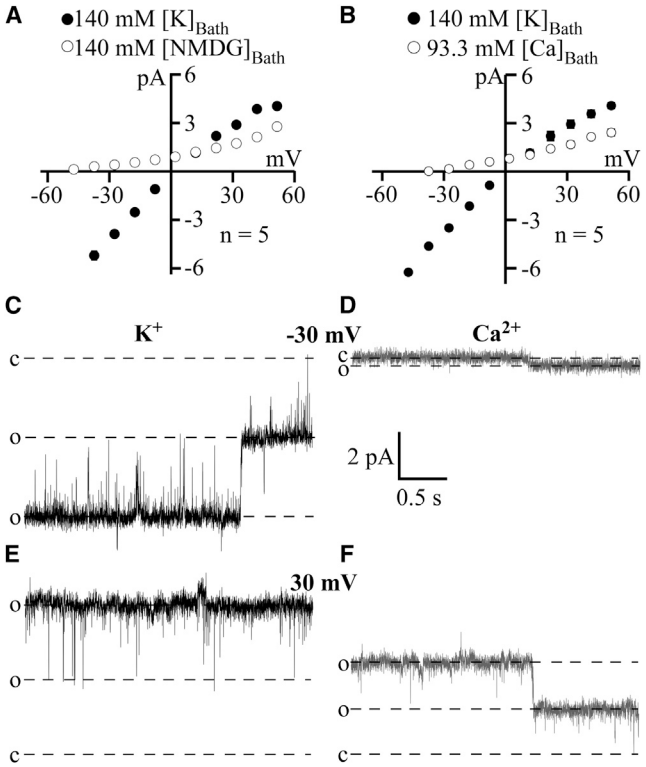

FIGURE 5 Effect of replacing K^+ ions with $NMDG^+$ or Ca^{2+} in the bath solution. (*A*) Average ($\pm$SE) i-V relationship obtained in K^+-based (*solid circles*) and $NMDG^+$-based (*open circles*) bath recording solution. Bath and pipette solutions contained 1.2 μM and 10 mM free Ca^{2+}, respectively. (*B*) Average ($\pm$SE) i-V relationships obtained in K^+-based (*solid circles*) and Ca^{2+}-based (*open circles*) bath recording solutions. (*C* and *D*) Representative channel traces recorded at -30 mV pipette potential in K^+-based (*C*) and Ca^{2+}-based (*D*) bath solutions. (*E* and *F*) Representative channel traces recorded at $+30$ mV pipette potential in K^+-based (*E*) and Ca^{2+}-based (*F*) bath solutions.

140 mM KCl in the bath solution was replaced with 93.3 mM $CaCl_2$ (to keep osmolarity constant). Under these conditions, only outward currents were observed at both negative and positive voltages ($n = 5$, Fig. 5, *B*, *D*, and *F*). Thus, although the outward permeation of internal K^+ ions was maintained, Ca^{2+} ions in the bath solution were unable to significantly permeate the channel. Interestingly, in the presence of 93.3 mM bath Ca^{2+}, the outward K^+ current at positive voltages was significantly reduced(Fig. 5, *B*, *D*, and *E*), suggesting an interaction between bath Ca^{2+} and internal K^+ within the channel pore.

Relative permeability to potassium, cesium, and sodium ions

We next determined the relative permeability of the small conductance nuclear channel to K^+ and Na^+. For these experiments, K^+ ions in the bath recording solution were replaced by Na^+ ions. Free Ca^{2+} concentrations remained 1.2 μM and 10 mM in the bath and pipette solutions,

respectively. Na^+ replacement resulted in a negative shift in the reversal potential to -24.6 ± 1.8 mV ($n = 5$) (Fig. 6 *A*), such that small inward currents carried by Na^+ ions were observed only at more negative voltages (Fig. 6, *A* and *C*). Based on the observed reversal potential in K^+ and Na^+ solutions, the calculated P_K/P_{Na} was 2.68 ± 0.21 ($n = 5$).

Cs^+ ions are known blockers of potassium-selective channels. However, NMCCs were found to exhibit significant permeability for Cs^+ ions (Fig. 7), though the unitary conductance when K^+ ions in the bath solution were replaced by Cs^+ ions (55.1 ± 4.8 pS, $n = 5$) was significantly reduced compared to that observed in symmetrical KCl (158 ± 7 pS, $n = 21$). In addition, the reversal potential with Cs^+ in the bath recording solution was shifted significantly to more negative potentials (-8.4 ± 0.5 mV, $n = 5$), such that the calculated P_K/P_{Cs} was 1.39 ± 0.03 ($n = 5$). Together, the results in Figs. 4–7 indicate that the channel in the nuclear inner membrane is selectively permeable to monovalent cations (NMCC).

An additional interesting observation was made in these monovalent cation replacement experiments. For both Cs^+ and Na^+, the i–V relationship was linearized at all test potentials, whereas a weakly inwardly rectifying i-V was a signature of the channel using symmetrical K^+-based recording solutions (Figs. 6 and 7). In addition, Na^+ ions in the bath did not alter outward K^+ currents at positive voltages, whereas outward currents were reduced during Cs^+ replacement in the bath solution. These findings could be explained by Cs^+ ions partially blocking K^+ outward currents through interactions with binding site(s) within the channel pore. Together these results indicate that the NMCC is a poorly selective potassium channel compared to that of classic voltage-gated potassium channels.

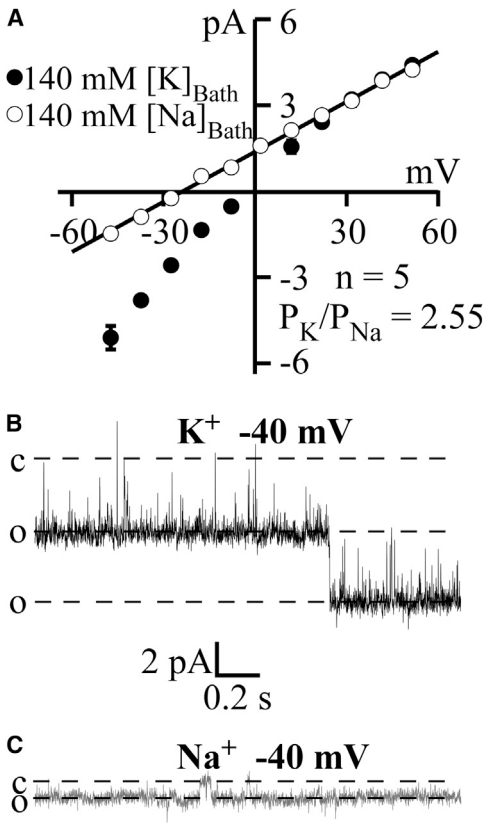

FIGURE 6 Selectivity of NMCC: K^+ vs. Na^+ ions. (*A*) Average (±SE) i–V relationships obtained in K^+-based (*solid circles*) and Na^+-based (*open circles*) bath solutions. Bath and pipette solutions contained 1.2 μM and 10 mM free Ca^{2+}, respectively. (*B* and *C*) Representative channel traces recorded at −40 mV pipette potential in K^+-based (*B*) and Na^+-based (*C*) bath solutions.

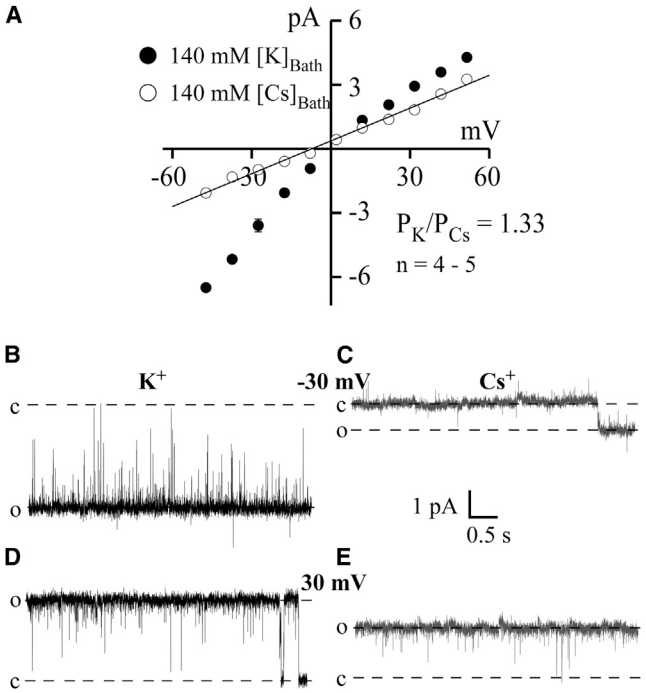

FIGURE 7 Selectivity of NMCCs: K^+ vs. Cs^+ ions. (*A*) Average (±SE) i–V relationships obtained in K^+-based (*solid circles*) and Cs^+-based (*open circles*) bath solutions. Bath and pipette solutions contained 1.2 μM and 10 mM free Ca^{2+}, respectively. (*B* and *C*) Representative single channel traces of activity recorded at −30 mV pipette potential in K^+-based (*B*) and in Na^+-based (*C*) bath solutions. (*D* and *E*) Representative single channel traces recorded at +30 mV pipette potential in K^+-based (*D*) and in Na^+-based (*E*) bath solutions.

Calcium ions decrease K^+ permeation of the NMCC

The results in Fig. 5 show that replacement of bath K^+ with Ca^{2+} resulted in a significant ($p < 0.05$) reduction in outward current carried by K^+ ions at voltages >10 mV. In addition, weak inward rectification was observed under conditions of symmetrical KCl even though the concentration of Ca^{2+} in the bath was >8000-fold lower than that of the intracellular solution (Fig. 3). Thus, we hypothesized that K^+ flux through NMCCs is modulated by Ca^{2+} ions in the bath recording solution. To test this hypothesis, we

completed single-channel measurements in symmetrical KCl and zero Ca^{2+} (0.1 mM K_2EGTA added), and in solutions in which the pipette Ca^{2+} concentration was 1.2 μM and the bath concentration was either 1.2 μM or 10 mM. In symmetrical zero Ca^{2+} ($n = 5$) and 1.2 μM Ca^{2+} ($n = 6$) solutions, the single-channel i-V relationships were nearly linear (Fig. 8 *A*). Outward currents were not significantly different between the two conditions at voltages higher than 30 mV ($p > 0.05$), whereas inward currents were bigger in zero Ca^{2+} symmetrical solution at voltages more negative than −30 mV. On the other hand, both inward and outward currents were significantly decreased ($p < 0.01$ except for V = −10 mV, $n = 5$–6) in the presence of 10 mM Ca^{2+} in the bath solution. We also determined the concentration-dependence for the Ca^{2+} inhibition of NMCC conductance by increasing the free Ca^{2+} concentration symmetrically in both pipette and bath solutions. Experimental data points were fitted by a standard Hill equation, which yielded numerical values for Hill coefficient = 0.9 and $[Ca]_{0.5} = 6.1$ mM (see Fig. 8 *D*). Due to potential problems associated with changes in osmolarity, we did not assess inhibition of NMCC conductance at symmetrical Ca^{2+} concentrations higher than 10 mM. As a result, the accuracy of the fit shown in Fig. 8 *D* is limited by the number of data points, particularly at higher Ca^{2+} concentrations. For symmetrical Ca^{2+} solutions, i-V curves were linear. On the other hand, the presence of 10 mM Ca^{2+} dramatically reduced the single-channel conductance to 71.5 ± 1.5 pS ($n = 8$), or to 38.8 ± 0.8% of the value obtained in zero Ca^{2+} symmetrical solution (Fig. 8 *C*). Based on these (Fig. 8) and other (Figs. 2, 5, and 6) results, we conclude that: i), asymmetric Ca^{2+} concentrations promote weak rectification; ii), weak rectification caused by asymmetric Ca^{2+} concentrations is only observed for K^+ and is absent for Cs^+ or Na^+; iii), K^+ conductance is reduced by increasing the Ca^{2+} concentration on either side of the channel; and iv), it is likely that Ca^{2+} ions compete with potassium ions for a single site within the NMCC pore.

DISCUSSION

To our knowledge, we provide the first direct biophysical characterization of ion channels in nuclei from adult skeletal muscle. Both an IP_3-sensitive, large conductance channel (325 pS) and a moderate conductance (158 pS) monovalent cationic channel were recorded from the inner membrane of nuclei isolated from adult skeletal muscle fibers. The NMCC exhibits a high, voltage-independent open probability, and as a result, the channel dwells in open state most of the time. Small monovalent cations such as potassium, sodium, and cesium readily permeate the channel with a relative permeability sequence of K> Cs > Na. However, large monovalent cations ($NMDG^+$) do not permeate the channel, suggesting that the narrowest part of the channel pore does not exceed ~7.3 Å, the mean diameter of $NMDG^+$ (47). Additionally, ion substitution experiments revealed that K^+ permeation through the NMCC is inhibited by Cs^+, but not Na^+, ions. The modest permeability preference for K^+ ions over Cs^+ and Na^+ ions and the inhibitory effect of Cs^+ ions on K^+ conduction suggest that the NMCC may be evolutionarily related to the potassium channel gene family. Finally, we also found that although Ca^{2+}

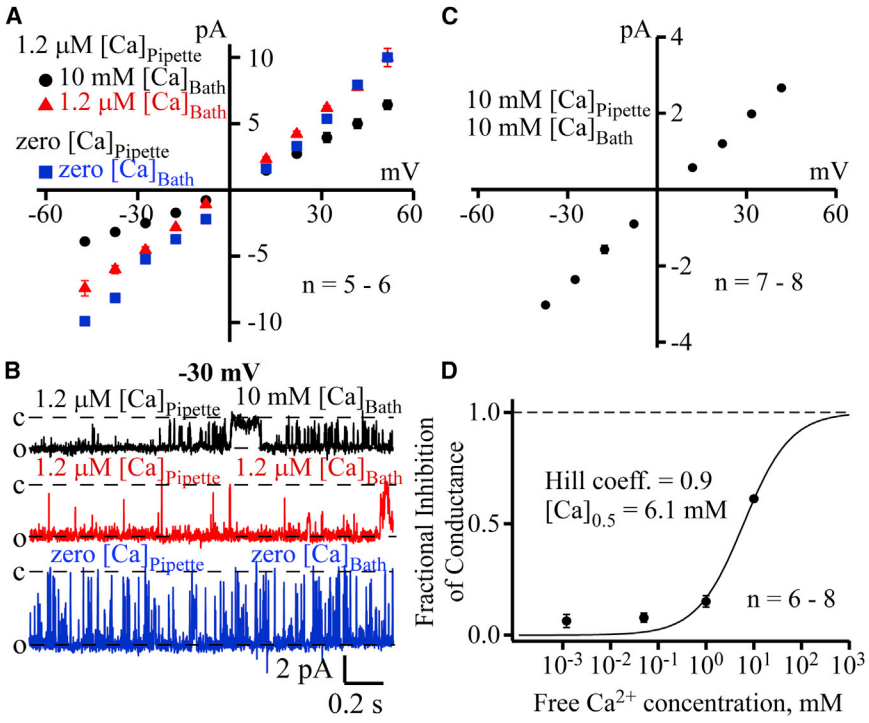

FIGURE 8 Effect of Ca^{2+} ions on K^+ currents. (*A*) Average (±SE) i–V relationships obtained in symmetrical zero Ca^{2+} solutions (*blue squares*) and either high Ca^{2+} (10 mM, *black solid circles*) or low Ca^{2+} (1.2 μM, *red triangles*) bath solutions with the patch pipette solution containing 1.2 μM Ca^{2+}. (*B*) Representative single-channel traces recorded at −30 mV pipette potential in high (*black*, *top trace*) and low (*red*, *middle trace*) Ca^{2+} bath solutions and 1.2 μM Ca^{2+} pipette solution, as well as using symmetrical zero Ca^{2+} solutions (*blue*, *bottom trace*). (*C*) Average (±SE) i–V relationships obtained in symmetrical 10 mM Ca^{2+} solutions. (*D*) Average (±SE) fractional inhibition of NMCC conductance—bath Ca^{2+} concentration dependence. The fractional inhibition of conductance was calculated as a ratio of the difference between the average maximal conductance measured in symmetrical zero Ca^{2+} solutions and measured conductance to the average maximal conductance measured in symmetrical zero Ca^{2+} solutions. Experimental data were fitted by a standard Hill equation (Hill coefficient = 0.9 and $[Ca]_{0.5}$ = 6.1 mM).

ions do not permeate NMCCs, they inhibit K^+ conductance through the channel, which is a unique effect of Ca^{2+} ions on NMCCs. Given that the Hill coefficient for Ca^{2+} inhibition of K^+ conductance was close to 1 (i.e., no cooperativity), Ca^{2+} ions appear to compete with potassium ions for a single site within the NMCC pore.

We also readily observed similar NMCC channel activity in nuclei isolated from *tibialis anterior* skeletal muscle (data not shown). Thus, the NMCC characterized here is likely to be an important nuclear ion channel that is widely expressed in skeletal muscle. However, NMCC expression may not be specific to skeletal muscle because a channel with similar properties was reported previously in Purkinje neurons (15). Specifically, Marchenko et al. (15) reported that nuclei from Purkinje neurons exhibit a large conductance monovalent cationic channel with high open probability, a preference for K^+ over Na^+ ions and inhibition by Ca^{2+} ions. Like that reported here, the detection frequency and number of active channels in each patch observed in Purkinje neurons was also very high, consistent with high channel expression (15). A second larger conductance NMCC channel was subsequently recorded from nuclei from Purkinje neurons (26), but this channel is distinct as it exhibits a prominent voltage-dependent change in channel P_o, which is not observed for the NMCC recorded from skeletal muscle We propose that the NMCC in skeletal muscle is related to the voltage-independent NMCC recorded from Purkinje neurons.

The molecular identity of the NMCC characterized here is currently unknown. However, given the properties of the NMCC, it is reasonable to speculate that the channel belongs to a family of molecularly unidentified monovalent cationic channels expressed in nuclei and the endo/sarcoplasmic reticulum (also known as SR K^+ channels). The presence of SR K^+ channels in the SR of skeletal and cardiac muscles has been known for almost four decades (48,49). These channels exhibit a similar conductance (49,50), preference for potassium over sodium (49), and modulation by Ca^{2+} ions (50), although SR K^+ channels typically exhibit a voltage-dependent P_o (51,52). Thus, it is possible that NMCCs are a member of the SR K^+ channels superfamily. As another possibility, the NMCC reported here could belong to the trimeric intracellular cation channel (TRIC) channel family, which likely do not belong to the SR K^+ channel family (53,54). Indeed, TRIC-A and TRIC-B channels are permeable to K^+ ions and have a single-channel conductance comparable to that of the NMCCs reported here (53,54). However, unlike NMCCs, TRIC-A and TRIC-B channels exhibit a significantly smaller and more voltage-dependent P_o (54). In addition, TRIC-B channels are blocked by application of 100 μM Ca^{2+} to the *trans* chamber and exhibit restored/increased activity when subsequently added to the *cis* chamber (54). Based on these differences, we conclude that NMCC activity recorded from skeletal muscle nuclei is unlikely to reflect TRIC-A or TRIC-B channel activity.

The absence of specific blockers and the unknown molecular identity of the NMCC make it difficult to evaluate the physiological role of these nuclear ion channels. Nevertheless, based on our results and those of previous studies, we hypothesize that NMCCs may serve several potential functions. First, the robust expression of NMCCs with a high and voltage-independent P_o is consistent with a role for these channels in equilibrating the K^+ concentration between the perinuclear space and nucleoplasm. Second, constitutive NMCC activity would prevent the development of an electrical potential across the nuclear membrane during Ca^{2+} release mediated by nuclear IP_3Rs and/or RyRs (for a review see (28)). Indeed, the nuclear envelope can serve as a significant local Ca^{2+} store in both skeletal and cardiac muscle cells (8,12,14,21,55) and we recorded IP_3-responsive channels in isolated muscle nuclei (Fig. 2). As NMCCs are expressed at high levels in the inner nuclear membrane, exhibit voltage-independent high P_o, and readily conduct K^+ ions, these channels are ideally suited to prevent the development of a membrane potential across the nuclear membrane, for example, during IP_3-mediated Ca^{2+} release. A similar role has been suggested for SR K^+ channels (56), TRIC channels (53,54), and other NMCCs (15,26). However, the low frequency of recording nuclear IP_3Rs in muscle nuclei raises the question of the relative physiological importance of this mechanism. Finally, nuclear potassium channel activity has also been suggested to influence gene expression via regulation of nucleoplasmic K^+ homeostasis (27). A more definitive determination of the physiological role of NMCCs in skeletal muscle will require the identification of specific channel inhibitors and/or the molecular determinants of the channel. We also examined several compounds known for their ability to block multiple channels. Specifically, neither 100 μM 2-APB nor 100 μM roscovitine significantly altered NMCC activity (data not shown). We also found that NMCC activity was not altered by 100 μM ryanodine (data not shown).

In conclusion, we provide the first, to our knowledge, direct functional identification of IP_3-activated channels and a biophysical characterization of NMCCs in the inner membrane of nuclei obtained from adult skeletal muscle fibers. The properties of the NMCCs (location, expression level, permeation, open probability) are well suited to both control perinuclear space-to-nucleoplasm K^+ concentrations and contribute to a counter current mechanism that limits the development of an electrical potential across the nuclear membrane during Ca^{2+} release from the perinuclear space. However, the precise physiological role of NMCCs in regulating gene transcription and nuclear Ca^{2+} signaling in muscle remains to be determined.

SUPPORTING MATERIAL

One figure is available at http://www.biophysj.org/biophysj/supplemental/S0006-3495(14)01004-2.

We thank Dr. Isabelle Marty (INSERM U836) for providing the triadin antibody used in this study. We also thank Drs. Ted B. Begenisich (University of Rochester) and David I. Yule (University of Rochester) for critical review of this manuscript.

This work was supported by a career development K01 award from National Institutes of Health (NIH) (AR060831 to V.Y.) and a research grant from the NIH (AR059646 to R.T.D.).

REFERENCES

1. Watson, M. L. 1955. The nuclear envelope; its structure and relation to cytoplasmic membranes. *J. Biophys. Biochem. Cytol.* 1:257–270.
2. Pappas, G. D. 1956. The fine structure of the nuclear envelope of Amoeba proteus. *J. Biophys. Biochem. Cytol.* 2 (4 Suppl):431–434.
3. Watson, M. L. 1959. Further observations on the nuclear envelope of the animal cell. *J. Biophys. Biochem. Cytol.* 6:147–156.
4. Bustamante, J. O. 2006. Current concepts in nuclear pore electrophysiology. *Can. J. Physiol. Pharmacol.* 84:347–365.
5. Bustamante, J. O., E. R. Michelette, …, T. J. McDonnell. 2000. Calcium, ATP and nuclear pore channel gating. *Pflugers Arch.* 439: 433–444.
6. Harris, P., and T. W. James. 1952. Electron microscope study of the nuclear membrane of *Amoeba proteus* in thin section. *Experientia.* 8:384–385.
7. Schatten, G., and M. Thoman. 1978. Nuclear surface complex as observed with the high resolution scanning electron microscope. Visualization of the membrane surfaces of the nuclear envelope and the nuclear cortex from *Xenopus laevis* oocytes. *J. Cell Biol.* 77:517–535.
8. Zima, A. V., D. J. Bare, …, L. A. Blatter. 2007. IP3-dependent nuclear Ca2+ signalling in the mammalian heart. *J. Physiol.* 584:601–611.
9. Gerasimenko, J. V., Y. Maruyama, …, O. V. Gerasimenko. 2003. NAADP mobilizes Ca2+ from a thapsigargin-sensitive store in the nuclear envelope by activating ryanodine receptors. *J. Cell Biol.* 163: 271–282.
10. Gerasimenko, J., Y. Maruyama, …, O. Gerasimenko. 2003. Calcium signalling in and around the nuclear envelope. *Biochem. Soc. Trans.* 31: 76–78.
11. Bezin, S., G. Charpentier, …, J. M. Cancela. 2008. Regulation of nuclear Ca2+ signaling by translocation of the Ca2+ messenger synthesizing enzyme ADP-ribosyl cyclase during neuronal depolarization. *J. Biol. Chem.* 283:27859–27870.
12. Marius, P., M. T. Guerra, …, M. F. Leite. 2006. Calcium release from ryanodine receptors in the nucleoplasmic reticulum. *Cell Calcium.* 39:65–73.
13. Escobar, M., C. Cardenas, …, C. Franzini-Armstrong. 2011. Structural evidence for perinuclear calcium microdomains in cardiac myocytes. *J. Mol. Cell. Cardiol.* 50:451–459.
14. Wu, X., T. Zhang, …, D. M. Bers. 2006. Local InsP3-dependent perinuclear Ca2+ signaling in cardiac myocyte excitation-transcription coupling. *J. Clin. Invest.* 116:675–682.
15. Marchenko, S. M., V. V. Yarotskyy, …, R. C. Thomas. 2005. Spontaneously active and InsP3-activated ion channels in cell nuclei from rat cerebellar Purkinje and granule neurones. *J. Physiol.* 565:897–910.
16. Stehno-Bittel, L., A. Lückhoff, and D. E. Clapham. 1995. Calcium release from the nucleus by InsP3 receptor channels. *Neuron.* 14: 163–167.
17. Mak, D. O., S. M. McBride, …, J. K. Foskett. 2003. Novel regulation of calcium inhibition of the inositol 1,4,5-trisphosphate receptor calcium-release channel. *J. Gen. Physiol.* 122:569–581.
18. Wagner, 2nd, L. E., and D. I. Yule. 2012. Differential regulation of the $InsP_3$ receptor type-1 and -2 single channel properties by $InsP_3$, Ca^{2+} and ATP. *J. Physiol.* 590:3245–3259.
19. Ionescu, L., K. H. Cheung, …, J. K. Foskett. 2006. Graded recruitment and inactivation of single InsP3 receptor Ca2+-release channels: implications for quantal [corrected] Ca2+release. *J. Physiol.* 573:645–662.
20. Rahman, T., and C. W. Taylor. 2010. Nuclear patch-clamp recording from inositol 1,4,5-trisphosphate receptors. *Methods Cell Biol.* 99: 199–224.
21. Kusnier, C., C. Cárdenas, …, E. Jaimovich. 2006. Single-channel recording of inositol trisphosphate receptor in the isolated nucleus of a muscle cell line. *Biol. Res.* 39:541–553.
22. Mak, D. O., H. Vais, …, J. K. Foskett. 2013. Patch-clamp electrophysiology of intracellular Ca2+ channels. *Cold Spring Harb. Protoc.* 2013:787–797.
23. Wagner, 2nd, L. E., L. A. Groom, …, D. I. Yule. 2014. Characterization of ryanodine receptor type 1 single channel activity using "on-nucleus" patch clamp. *Cell Calcium.* 56:96–107.
24. Longin, A. S., P. Mezin, …, J. Verdetti. 1997. Presence of zinc and calcium permeant channels in the inner membrane of the nuclear envelope. *Biochem. Biophys. Res. Commun.* 235:236–241.
25. Tabares, L., M. Mazzanti, and D. E. Clapham. 1991. Chloride channels in the nuclear membrane. *J. Membr. Biol.* 123:49–54.
26. Fedorenko, O., V. Yarotskyy, …, S. Marchenko. 2010. The large-conductance ion channels in the nuclear envelope of central neurons. *Pflugers Arch.* 460:1045–1050.
27. Chen, Y., A. Sánchez, …, W. Stühmer. 2011. Functional K(v)10.1 channels localize to the inner nuclear membrane. *PLoS ONE.* 6:e19257.
28. Rousseau, E., C. Michaud, …, A. Decrouy. 1996. Reconstitution of ionic channels from inner and outer membranes of mammalian cardiac nuclei. *Biophys. J.* 70:703–714.
29. Mazzanti, M., J. O. Bustamante, and H. Oberleithner. 2001. Electrical dimension of the nuclear envelope. *Physiol. Rev.* 81:1–19.
30. Humbert, J. P., N. Matter, …, A. N. Malviya. 1996. Inositol 1,4,5-trisphosphate receptor is located to the inner nuclear membrane vindicating regulation of nuclear calcium signaling by inositol 1,4,5-trisphosphate. Discrete distribution of inositol phosphate receptors to inner and outer nuclear membranes. *J. Biol. Chem.* 271:478–485.
31. Valenzuela, S. M., M. Mazzanti, …, S. N. Breit. 2000. The nuclear chloride ion channel NCC27 is involved in regulation of the cell cycle. *J. Physiol.* 529:541–552.
32. Franco-Obregón, A., H. W. Wang, and D. E. Clapham. 2000. Distinct ion channel classes are expressed on the outer nuclear envelope of T- and B-lymphocyte cell lines. *Biophys. J.* 79:202–214.
33. Juretić, N., U. Urzúa, …, N. Riveros. 2007. Differential gene expression in skeletal muscle cells after membrane depolarization. *J. Cell. Physiol.* 210:819–830.
34. Cárdenas, C., N. Juretić, …, E. Jaimovich. 2010. Abnormal distribution of inositol 1,4,5-trisphosphate receptors in human muscle can be related to altered calcium signals and gene expression in Duchenne dystrophy-derived cells. *FASEB J.* 24:3210–3221.
35. Shen, T., Y. Liu, …, M. F. Schneider. 2010. DNA binding sites target nuclear NFATc1 to heterochromatin regions in adult skeletal muscle fibers. *Histochem. Cell Biol.* 134:387–402.
36. Liu, Y., Z. Cseresnyés, …, M. F. Schneider. 2001. Activity-dependent nuclear translocation and intranuclear distribution of NFATc in adult skeletal muscle fibers. *J. Cell Biol.* 155:27–39.
37. Lillis, S., S. Abbs, …, H. Jungbluth. 2012. Clinical utility gene card for: multi-minicore disease. *Eur. J. Hum. Genet.* 20:20.
38. Blaauw, B., P. Del Piccolo, …, S. Schiaffino. 2012. No evidence for inositol 1,4,5-trisphosphate-dependent Ca2+ release in isolated fibers of adult mouse skeletal muscle. *J. Gen. Physiol.* 140:235–241.
39. Tjondrokoesoemo, A., N. Li, …, J. Ma. 2013. Type 1 inositol (1,4,5)-trisphosphate receptor activates ryanodine receptor 1 to mediate calcium spark signaling in adult mammalian skeletal muscle. *J. Biol. Chem.* 288:2103–2109.

40. Wang, X., N. Weisleder, …, J. Ma. 2005. Uncontrolled calcium sparks act as a dystrophic signal for mammalian skeletal muscle. *Nat. Cell Biol.* 7:525–530.

41. Beam, K. G., and C. M. Knudson. 1988. Calcium currents in embryonic and neonatal mammalian skeletal muscle. *J. Gen. Physiol.* 91:781–798.

42. Goonasekera, S. A., N. A. Beard, …, R. T. Dirksen. 2007. Triadin binding to the C-terminal luminal loop of the ryanodine receptor is important for skeletal muscle excitation contraction coupling. *J. Gen. Physiol.* 130:365–378.

43. Marty, I., M. Robert, …, M. Villaz. 1995. Localization of the N-terminal and C-terminal ends of triadin with respect to the sarcoplasmic reticulum membrane of rabbit skeletal muscle. *Biochem. J.* 307:769–774.

44. Mak, D. O., H. Vais, …, J. K. Foskett. 2013. Isolating nuclei from cultured cells for patch-clamp electrophysiology of intracellular Ca(2+) channels. *Cold Spring Harb. Protoc.* 2013:880–884.

45. Mak, D. O., and J. K. Foskett. 1998. Effects of divalent cations on single-channel conduction properties of *Xenopus* IP3 receptor. *Am. J. Physiol.* 275:C179–C188.

46. Mak, D. O., S. McBride, …, J. K. Foskett. 2000. Single-channel properties in endoplasmic reticulum membrane of recombinant type 3 inositol trisphosphate receptor. *J. Gen. Physiol.* 115:241–256.

47. Villarroel, A., N. Burnashev, and B. Sakmann. 1995. Dimensions of the narrow portion of a recombinant NMDA receptor channel. *Biophys. J.* 68:866–875.

48. Miller, C., and E. Racker. 1976. Ca++-induced fusion of fragmented sarcoplasmic reticulum with artificial planar bilayers. *J. Membr. Biol.* 30:283–300.

49. Tomlins, B., A. J. Williams, and R. A. Montgomery. 1984. The characterization of a monovalent cation-selective channel of mammalian cardiac muscle sarcoplasmic reticulum. *J. Membr. Biol.* 80:191–199.

50. Uehara, A., M. Yasukochi, and I. Imanaga. 1994. Calcium modulation of single SR potassium channel currents in heart muscle. *J. Mol. Cell. Cardiol.* 26:195–202.

51. Picard, L., K. Côté, …, E. Rousseau. 2002. Sarcoplasmic reticulum K(+) channels from human and sheep atrial cells display a specific electro-pharmacological profile. *J. Mol. Cell. Cardiol.* 34:1163–1172.

52. Côté, K., S. Proteau, …, E. Rousseau. 2000. Characterization of the sarcoplasmic reticulum k(+) and Ca(2+)-release channel-ryanodine receptor-in human atrial cells. *J. Mol. Cell. Cardiol.* 32:2051–2063.

53. Yazawa, M., C. Ferrante, …, H. Takeshima. 2007. TRIC channels are essential for Ca2+ handling in intracellular stores. *Nature.* 448:78–82.

54. Pitt, S. J., K. H. Park, …, R. Sitsapesan. 2010. Charade of the SR K+-channel: two ion-channels, TRIC-A and TRIC-B, masquerade as a single K+-channel. *Biophys. J.* 99:417–426.

55. Cárdenas, C., J. L. Liberona, …, E. Jaimovich. 2005. Nuclear inositol 1,4,5-trisphosphate receptors regulate local Ca2+ transients and modulate cAMP response element binding protein phosphorylation. *J. Cell Sci.* 118:3131–3140.

56. Meissner, G., and D. McKinley. 1982. Permeability of canine cardiac sarcoplasmic reticulum vesicles to K+, Na+, H+, and Cl-. *J. Biol. Chem.* 257:7704–7711.